Development of a Novel Sensor Based on Polypyrrole Doped with Potassium Hexacyanoferrate (II) for Detection of L-Tryptophan in Pharmaceutics

Ancuța Dinu 🆔 **and Constantin Apetrei** *🆔

Department of Chemistry, Phyiscs and Environment, Faculty of Science and Environment,
"Dunărea de Jos" University of Galati, 47 Domnească Street, RO-800008 Galati, Romania; ancuta.dinu@ugal.ro
* Correspondence: apetreic@ugal.ro; Tel.: +40-727-580-914

Abstract: This study describes the development of a new sensor with applicability in the determination and quantification of yjr essential amino acid (AA) L-tryptophan (L-TRP) from pharmaceutical products. The proposed sensor is based on a carbon screen-printed electrode (SPCE) modified with the conductor polymer polypyrrole (PPy) doped with potassium hexacyanoferrate (II) (FeCN). For the modification of the SPCE with the PPy doped with FeCN, the chronoamperometry (CA) method was used. For the study of the electrochemical behavior and the sensitive properties of the sensor when detecting L-TRP, the cyclic voltammetry (CV) method was used. This developed electrode has shown a high sensibility, a low detection limit (LOD) of up to 1.05×10^{-7} M, a quantification limit (LOQ) equal to 3.51×10^{-7} M and a wide linearity range between 3.3×10^{-7} M and 1.06×10^{-5} M. The analytical performances of the device were studied for the detection of AA L-TRP from pharmaceutical products, obtaining excellent results. The validation of the electroanalytical method was performed by using the standard method with good results.

Keywords: L-tryptophan; polypyrrole; sensor; amino acid; cyclic voltammetry; chronoamperometry

1. Introduction

Tryptophan (TRP), with the molecular formula $C_{11}H_{11}N_2O_2$, is a well-known substance, being part of the essential AA category that cannot be produced naturally by the human body [1]. This chemical compound is hardly found in its natural form, which makes it expensive. TRP is the precursor of the neurotransmitter serotonin, the neurohormone melatonin and niacin (or the PP vitamin) [2]. TRP works as a chemical precursor for 5-hydroxytryptophan (5-HTP), as well as a coenzyme for the nicotinamide adenine dinucleotide (NAD) and nicotinamide adenine dinucleotide phosphate (NADP) [3]. In Figure 1, the pathway for the biosynthesis of TRP is presented.

Being a chiral molecule, TRP is found under two isomers—a natural form (L-TRP) and a synthetic one (D-TRP)—with both forms being almost identical in their physical-chemical properties, a fact which leads to difficulties in distinguishing them [2,4]. In the literature, there are multiple methods explained on how to identify enantiomers [5–7]. The chemical structures of the two enantiomers can be seen in Figure 2.

TRP is most frequently found in food, such as chicken and turkey meat, peanut tofu, sesame seeds, eggs, sunflower seeds, pumpkin seeds, soy and chocolate, as well as in dairy products and pharmaceutical products available on the market with different concentrations of TRP [8]. The recommended dose of TRP by the World Health Organization is 4 mg/kg/day [9]. In the case of improper metabolism of TRP, hallucinations and disappointment can take place, which is why a deficiency or an excess of L-TRP could lead to problems that could affect the nervous system's health [10]. Additionally, phytoproducts or nutraceuticals containing TRP can be administered in the case of depression caused by the new coronavirus (SARS-CoV-2) [11]. For these reasons, L-TRP was selected to be

detected as fast as possible from pharmaceutics by a new device: a compound which contributes to preventing neuropsychiatric disorders led by the lack of AA, such as depression [12], anxiety [13], insomnia [14], attention deficit hyperactivity disorder (ADHD) [15], the premenstrual syndrome [16] and Parkinson's disease [17].
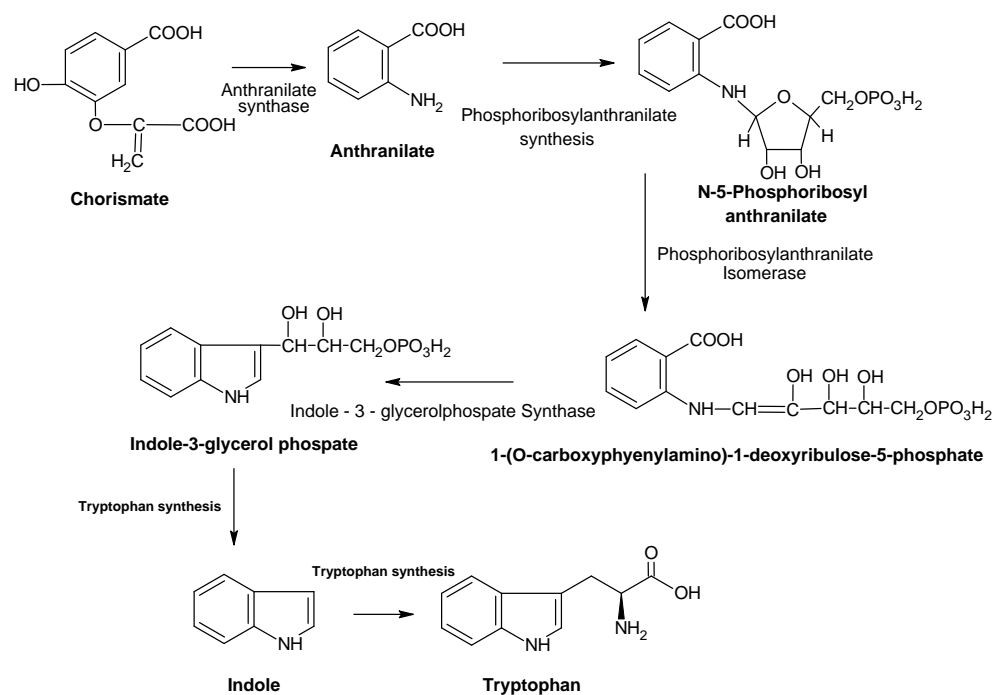

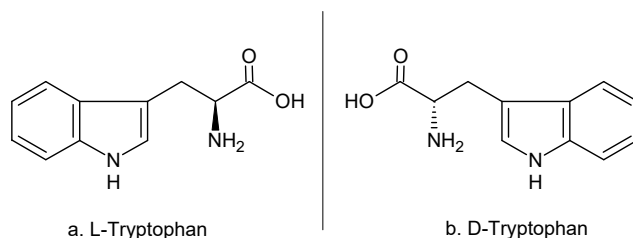**Figure 1.** The pathway for the synthesis of TRP (adapted from [3]).

Figure 2. The chemical structure of the two enantiomers. (adapted from [5]).

The physicochemical properties of TRP are very important, being important features for accurate detection. Over time, a variety of methods for the detection of L-TRP and its derivatives were tested, as can be seen in Table 1.

Table 1. Physicochemical methods used for L-TRP detection.

The Detection Method	Reference
Chromatography	[18]
Spectroscopy	[19–22]
Colorimetry	[23]
High-performance liquid chromatography (HPLC)	[19,21,24,25]
Capillary electrophoresis	[26]
Chemiluminescence	[27]
Atomic force spectroscopy	[28]

These methods proved to be expensive and required time to obtain the results, facts that led to more versatile methods that were based on electroanalysis using sensors [29] and

biosensors for the much more simple, sensible and selective detection of TRP from pharmaceutical, biological and food products, using electrochemical detection methods such as CV [30,31], differential pulse voltammetry (DPV) [20,30] and square wave voltammetry (SWV) [9,32].

The main sensors developed over the years, used for the determination of the L-TRP quantity, sensitive materials and electroanalytical performance characteristics, are presented in Table 2.

Table 2. The sensitive material, the detection limit and the linear range of the main sensors for the determination of L-TRP through electrochemical methods.

Electrode Materials	The Detection Technique	The Detection Limit	The Linear Range	Reference
Cu$_2$O-ERGO/GCE (nanocomposite of cuprous oxide and electrochemically reduced graphene oxide)	CV [1], SWV [2]	0.01×10^{-6} M	0.02–20×10^{-6} M	[9]
Nafion-MIP-MWCNTs@IL/GCE (molecularly imprinted copolymer of dual functional monomers and ionic liquid (1-butyl-3-methylimidazolium hexafluorophosphate) functionalized multi-walled carbon nanotubes)	LSV [3], DPV [4]	6×10^{-9} M	8×10^{-9}–26×10^{-6} M	[33]
PVP-GR/GCE (glassy carbon electrode modified with polyvinylpyrrolidonefunctionalized graphene/glassy carbon electrode)	CV	0.01×10^{-6} M	0.06–10.0×10^{-6} M and 10.0–100.0×10^{-6} M	[34]
GR/PEDOT:PSS/GCE (glassy carbon electrode modifed with exfoliated graphene and poly (3,4-ethylenedioxythiophene): poly (styrene sulfonate)	CV	0.015×10^{-6} M	0.1–100×10^{-6} M and 100–1000×10^{-6} M	[35]
PPy/FeCN/SPCE	CV, CA [5]	1.05×10^{-7} M	3.3×10^{-7} M–1.06×10^{-5} M	This work

[1] Cyclic voltammetry. [2] Square wave voltammetry. [3] Linear sweep voltammetry. [4] Differential pulse voltammetry. [5] Chronoamperometry.

In addition, the novel sensor developed in this study is presented in Table 2, developed using a conducting polymer doped with an electroactive compound (PPy and ferrocyanide). The device obtained a lower detection limit and a wider linearity range compared with the other sensors, proving more sensitive L-TRP detection.

The selected polymer for the modification of the sensor was the PPy so that this might present a series of characteristics and advantages that led to higher performance of the sensor, including improved stability and sensibility and high electrical conductivity, malleability and biocompatibility [36]. The doping of PPy by electropolymerization with the help of CA is the usual electrochemical synthesis method, used in improving properties such as stability, conductivity, fast electron transfers and permeability so that this type of sensor could be applied in multiple fields, such as chemistry, pharmaceutics, medicine, the food industry and biology [37,38]. In the literature, for the synthesis of PPy and its doping, certain electrochemical methods were used often, namely CA, CV and chronopotentiometry (CP) [37]. The doping agent of PPy selected for this study was FeCN, which offered to the sensor good sensitivity, reproducibility and stability.

The analytical performances of the sensor developed in this study were evaluated in model solutions and in solutions obtained through pharmaceutical products with distinct concentrations of L-TRP from different manufacturers, followed by validation with the standard method based on Fourier-transform infrared (FT-IR) spectroscopy.

2. Materials and Methods

2.1. Reagents and Solutions

L-TRP ($\geq$98%), potassium chloride ($\geq$99.0%), potassium hexacyanoferrate (II) trihydrate ($\geq$99.5%) and pyrrole (98%) were purchased from Sigma-Aldrich (St. Louis, MO, USA).

All reagents were of analytical grade, and all of the solutions within this study were prepared in ultrapure water (18.3 MΩ $\times$ cm, Milli—Q Simplicity$^\circledR$ Water Purification System from Millipore Corporation) (Bedford, MA, USA).

Potassium chloride (KCI) was used as an electrolyte support, the concentration being somewhere around 0.1 M in all of the analyzed solutions.

In order to validate the obtained results with the modified sensor, two pharmaceutical products that contained L-TRP—Sleep Optimizer SOLARAY (150 mg tryptophan) and Cebrium NEUROPHARMA (1.02 mg tryptophan)—were used. The preparation of the solutions was realized every day, and only freshly solutions were used in the electrochemical determinations.

2.2. Instrumentation

For the modification and characterization of the sensors, two potentiostats were used: a model 263A EG&G potentiostat/galvanostat (Princeton Applied Research, Oak Ridge, TN, USA) controlled by ECHEM software and a Biologic SP 150 potentiostat/galvanostat (Bio-Logic Science Instruments SAS, Seyssinet-Pariset, France) controlled by EC—Lab Express software. The first potentiostat was used for modification of the electrodes with PPy (polypyrrole) through the CA (chronoamperometry) method, and the second potentiostat was used for obtaining the electrochemical responses of the sensors using the CV (cyclic voltammetry) method.

The analysis of the obtained data from chronoamperograms and voltammograms was carried out using Origin (version 6.0) and Microsoft Office Excel (version 2007) software.

The electrochemical cell used had a capacity of 15 mL, and the electrode system was formed from the reference electrode and the counter electrode integrated into the sensor device (counter electrode: carbon; reference electrode: Ag/AgCl). The working electrode was the modified electrode with PPy. For modification, an SPCE (DRP-C110 working in a solution) was used, which was purchased from Dropsens (www.dropsens.com, accessed on 20 May 2021).

For the TRP study, the FT-IR method was used with the Bruker ALPHA FT-IR spectrophotometer (BrukerOptik GmbH, Ettlingen, Germany), controlled by OPUS software (BrukerOptik GmbH, Ettlingen, Germany). An Elmasonic S10H ultrasonic bath was used for the dissolution of the compounds and the homogenization of the solutions. In addition, analytical balance, volumetric flasks, pipettes and micropipettes were used for weighting the solid samples and for the preparation of the solutions.

2.3. Preparation of PPy/FeCN/SPCE

For the deposition of PPy on the SPCE, a solution of 0.1 M pyrrole and 0.1 M FeCN was prepared. Then, 15 mL of the solution was introduced in the electrochemical cell, and in the solution, the DRP-C110 electrode was immersed, making connections to the EG&G potentiostat. The deposition of the PPy thin film in the presence of the doping agent was realized with the help of the CA method, employing the following working parameters: a potential of 0.8 V and a deposition time of 90 s. The obtained chronoamperograms related to the electropolymerization processes are presented in Figure 3 in two forms: the current's dependence on the time (Figure 3A) and the dependence of the electric charge on the time (Figure 3B). These chronoamperograms were recorded for three different sensors developed in the same experimental conditions.
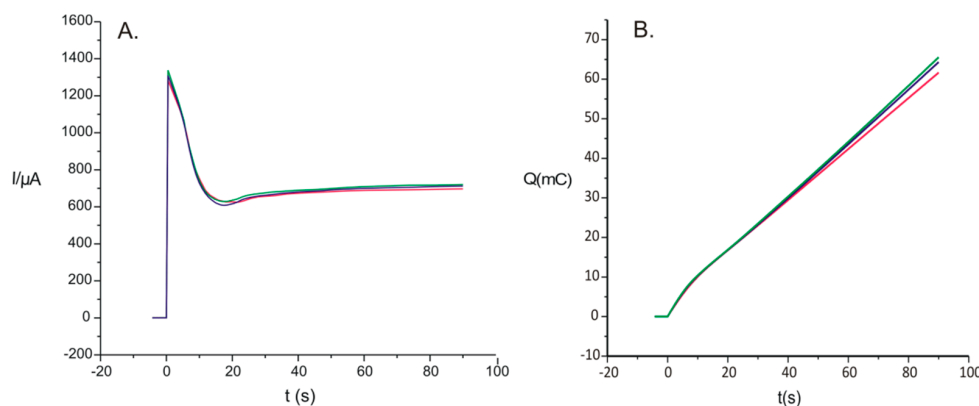
Figure 3. (**A**) Dependence of current (I) versus time (t) of curves registered in the electrosynthesis process of PPy /FeCN films at 0.8 V for 90 s. (**B**) Charge (Q) versus time (t) when PPy underwent electrosynthesis in the presence of FeCN for three replicate sensors.

The chronoamperograms presented in Figure 3A,B were compared for the purpose of determination of the reproducibility of electropolymerization. There were small differences, with a coefficient of variation of 2.9% between the chronoamperograms of the sensors prepared in the same conditions.

Additionally, from the chronoamperograms recorded during electropolymerization, the thickness of the PPy layer deposited on the surface of the carbon electrode was determined with the help of the ratio between the product of the oxidation load (Q), the molecular mass of the monomer (M = 67.0892 g/mol), the product of the number of electrons (n) involved with the Faraday constant (F = 96,485.33 C/mol), the active surface of the sensor (A) and the polymer's density (ρ_{PPy} = 1.5 g/cm^3) using the following equation [39]:

$$d = QM_w / nFA\rho \tag{1}$$

The value of d obtained for the PPy/FeCN sensor was of 0.203 μm, which demonstrates that the electrodeposition was facilitated in the presence of the doping agent FeCN, and the thickness of this film was optimal for the detection of L-TRP.

2.4. Samples Tested

Two pharmaceutical products that one can get without a medical prescription were tested with the PPy/FeCN sensor. Each one of them had different contents of the AA of L-TRP, and they came from different manufacturers, such as Cebrium (EVER NEURO PHARMA) (1.02 mg L-tryptophan per capsule) and Sleep Optimizer (SECOM) (150 mg L-tryptophan per capsule). Cebrium is a product that contains the following AAs besides L-TRP: glutamic acid, leucine, lysine, aspartic acid, arginine, phenylalanine, serine, threonine, valine, isoleucine, tyrosine, histidine and methionine.

Using the contents of the capsules mentioned earlier, they were prepared for different solutions with the purpose of analyzing three different concentrations for every sample, dissolved in 0.1 M KCl. The electrochemical analysis of the products was realized with the help of the CV method at a potential range between −1.0 V and +0.5 V at a scanning rate of 0.1 V × s^{-1}.

The standard FT-IR method was used for validating the obtained results of the electroanalytical method developed in this study. The IR spectra obtained for the two pharmaceutics with the Bruker ALPHA (BrukerOptik GmbH, Ettlingen, Germany) spectrophotometer ranged between 4000 and 500 cm^{-1}. The resolution of the recorded spectra was 4 cm^{-1} within 32 scans. The ZnSe crystals of this spectrophotometer were cleaned with ultra-pure water and isopropanol before adding the samples to be analyzed, eliminating possible impurities.

3. Results and Discussions

The sensor's analysis was performed with a Biologic SP 150 potentiostat/galvanostat by the CV electrochemical method in the potential range between -1.0 V and $+0.5$ V.

3.1. The Electrochemical Behavior of the Unmodified DRP-110 Electrode in 0.1 M KCl–10^{-3} M L-TRP Solution

In order to prove the device's efficiency developed in this study, few preliminary analyses were carried out. Before the modification, the SPCE was immersed in a solution of 0.1 M KCl–10^{-3} M L-TRP, and the cyclic voltamogram was recorded, comparing the results obtained from the unmodified sensor and the results from the modified sensor with PPy/FeCN. Using the electrochemical parameters mentioned above, the voltamogram obtained with the unmodified sensor at a scan rate of 0.1 V $\times$ s^{-1} is presented in Figure 4.
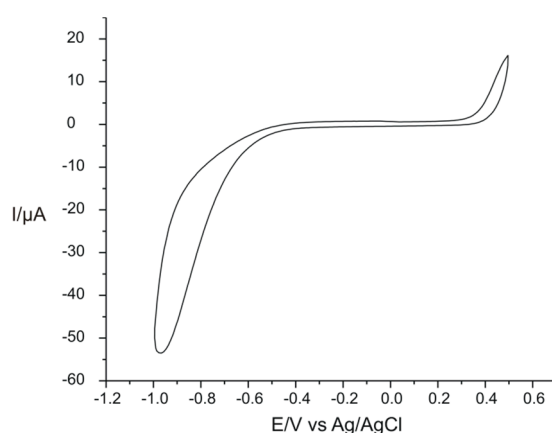

Figure 4. The electrochemical behavior of the unmodified sensor in a double solution of 0.1 M KCl and 10^{-3} M L-TRP at a scan rate of 0.1 V $\times$ s^{-1}.

It can be seen that the unmodified electrode did not show peaks in the studied potential range, and the background current was reduced. Therefore, the electrode's modification was necessary for L-TRP detection.

3.2. The Electrochemical Response of the Modified Electrode with PPy/FeCN in a 0.1 M KCl Solution and in a 0.1 M KCl–10^{-3} M L-TRP Double Solution

After the modification with PPy/FeCN, the electrochemical behavior of the sensor was initially analyzed in a 0.1 M KCl solution to observe the redox processes of PPy and the ferrocyanide ion included in the polymer matrix. In order to stabilize the sensor's signal in the electrolyte solution, six consecutive cycles were recorded. After this stage, the signal became stable. Using the same electrochemical parameters and going through the same stages with a scan rate of 0.1 V $\times$ s^{-1} and a potential range between -1.0 V and $+0.5$ V, the PPy/FeCN/SPCE sensor was analyzed in a double solution of 0.1 M KCl and 10^{-3} M L-TRP, where it was observed that the potentials and currents of the peaks, as well as their forms, were influenced by the presence of AA L-TRP through shifting the potentials of the peaks, increasing their currents, especially in the case of cathodic peaks. Figure 5 shows the stable signal of the modified sensor immersed in 0.1 M KCl overlayed with the stable signal of PPy/FeCN/SPCE immersed in a double solution of 0.1 M KCl and 10^{-3} M L-TRP.

Both in the first solution and in the second solution, we can see two pairs of peaks; the first pair (I) corresponded to the redox processes of the PPy polymer, and the second pair of peaks (II) was due to the redox processes of the doping ion immobilized in the polymer matrix (FeCN) [40]. The important difference between the two voltammograms was represented by the presence of AA L-TRP in the second solution, in which the electrode was immersed in the 10^{-3} M L-TRP solution, having as an electrolyte support 0.1 M KCl.

This difference can be seen in Table 3, which includes the potentials and peak currents for both redox systems obtained from the cyclic voltammograms recorded with the PPy/FeCN sensor in the two analyzed solutions.
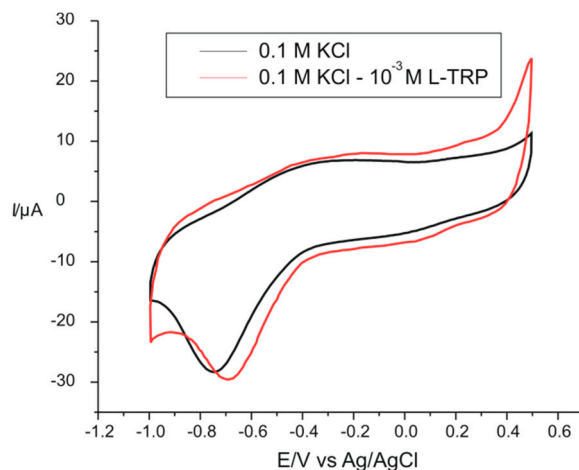

Figure 5. Electrochemical response of PPy/FeCN sensor immersed in a 0.1 M KCl solution (black line) and in a double solution 0.1 M KCl–10^{-3} M L-TRP (red line) at 0.1 V $\times$ s^{-1}.

Table 3. The potentials and currents of the peaks of PPy-modified sensors and immersed in a 0.1 M KCl solution and in a double solution 0.1 M KCl–10^{-3} M L-TRP at scan rate of 0.1 V $\times$ s^{-1}.

Sensor	Solution		Electrochemical Parameters					
			E_{pa} [1] (V)	E_{pc} [2] (V)	ΔE [3] (V)	I_{pa} [4] (μA)	I_{pc} [5] (μA)	I_{pc}/I_{pa}
PPy/FeCN/SPCE	0.1 M KCl	Redox system I	−0.27	−0.74	−1.01	6.76	−28.33	4.19
		Redox system II	0.16	0.03	0.13	7.07	−4.94	0.69
PPy/FeCN/SPCE	0.1 M KCl–10^{-3} M L-TRP	Redox system I	−0.31	−0.78	0.47	6.81	−31.24	4.58
		Redox system II	0.22	0.06	0.16	9.33	−7.70	0.82

[1] Potential of the anodic peak. [2] Potential of the cathodic peak. [3] $\Delta E = E_{pa} - E_{pc}$. [4] Current of the anodic peak. [5] Current of the cathodic peak.

It was proven by the obtained results that the PPy/FeCN/SPCE sensor could be useful for the detection of L-TRP, similar to reports from other scientific works, with the mention that some characteristics of the electrode (such as the electrode's surface and the modifier material) and some electrochemical parameters (the potential field and the scan rate) were not the same.

The TRP showed redox activity, being oxidized to 2-amino-3- (5-oxo-3,5-dihydro-2H-indol-3-yl) propionic acid, with two protons and two electrons involved in the oxidation reaction [41]. The mechanism of the oxidation reaction is illustrated in Figure 6.
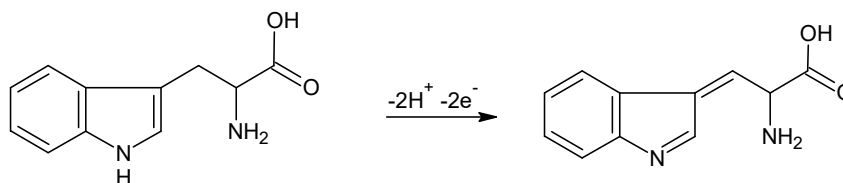

Figure 6. Process of the electrochemical oxidation of L-TRP (adapted from [35]).

3.3. The Influence of the Scan Rate on the Sensor Responses Immersed in a 0.1 M KCl and 10^{-3} M L-TRP Solution

The proposed sensor for L-TRP detection was immersed in the double solution of 10^{-3} M L-TRP and 0.1 M KCl, recording cyclic voltammograms at 10 different scan rates, and the results are shown in Figure 7A. The scan rates varied between 0.1 and 1.0 V $\times$ s^{-1}. Playing an important role for the electrochemical measurements, the scan rate influenced the redox processes. In the case of the intensity of the cathodic peak for the PPy/FeCN electrode, a linear dependence with the scan rate was observed. That way, the determining factor of rate could be established. From the linear relationship between the intensity of the cathodic peak and the scan rate (Figure 7B), it was concluded that the redox process from the level of the sensitive element was controled by the electron transfer from the electrochemical reaction. The linear fitting equation was $I_{pc} = 0.87268 \times v - 20.486$, and the coefficient of determination (R^2) was 0.9901, showing good quality for the linear regression model.
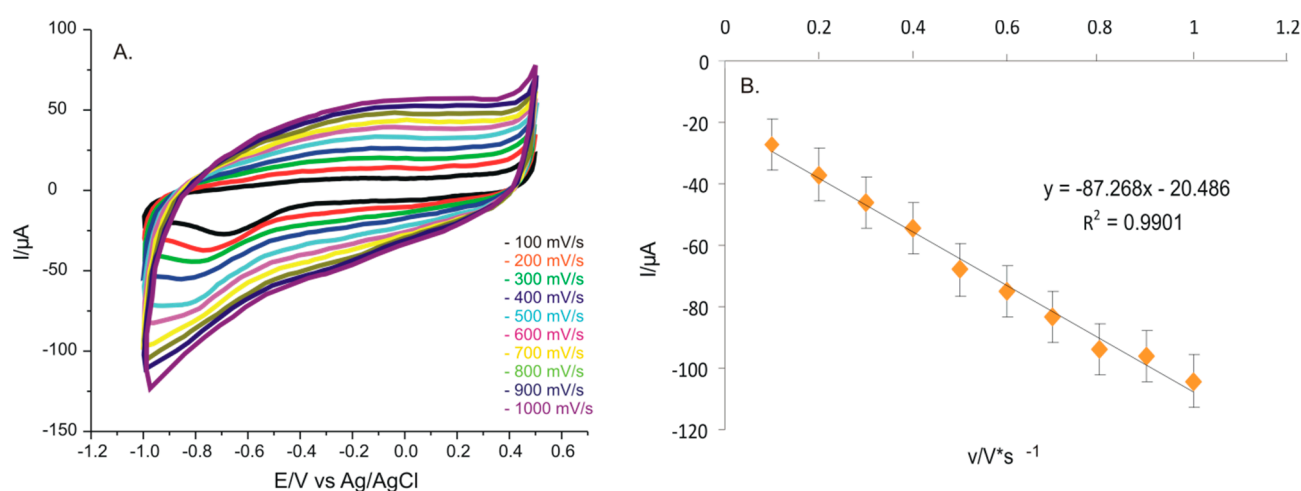

Figure 7. (**A**) CVs of PPy/FeCN/SPCE sensor immersed in a 0.1 M KCl and 10^{-3} M L-TRP solution at scan rates between 0.1 and 1.0 V $\times$ s^{-1}. (**B**) The plot of the linear dependence between I_{pc} and the scan rate.

Laviron's equation, $I_{pc} = n^2 F^2 \Gamma Av/4 RT$ (where *n* is the number of transfered electrons, F is Faraday's constant (F = 96 485 C mol^{-1}), A is the covered surface expressed in mol $\times$ cm^{-2}, v is the scan rate, R is the universal gas constant (R = 8.314 J mol^{-1} K^{-1}) and T is the absolute temperature (T = 298 K)), allowing the calculation of the degree of coverage on the electrode surface with active centers (Γ), that being 1.76×10^{-10} mol $\times$ cm^{-2}, considering the linear equation between the scan rate and the current of the most intense cathodic peak. This value was close to the results reported in the literature [42].

In conclusion, the modified elctrode with PPy/FeCN demonstrated a high sensitivity for L-TRP from the solution to be analyzed, the peaks being more intense with the increasing scan rate.

3.4. Influence of the Concentration on Responses of the Sensor Immersed in a 0.1 M KCl and 10^{-3} M L-TRP Solution: Calibration Curve

The concentration of the analyzed solution proved to be important for the electrochemical responses of the PPy/FeCN sensor, used in the present study solutions with different concentrations of L-TRP dissolved in a solution of 0.1 M KCl. The concentration range studied was between 3.33×10^{-7} M and 2.72×10^{-5} M, recording the cyclic voltamograms presented in Figure 8A with a scan rate of 0.1 V $\times$ s^{-1} and in the potential range between -1.0 V and $+0.5$ V. Figure 8B presents the most intense cathodic peak currents as a function of the L-TRP concentration. The calibration curve was obtained from the dependence of the cathodic current on the concentration (Figure 8C). The linearity range (Figure 8D) was

observed to be between 3.3×10^{-7} M and 1.06×10^{-5} M, and the calibration equation and the calculated values of the LOD and LOQ are reported in Table 4.
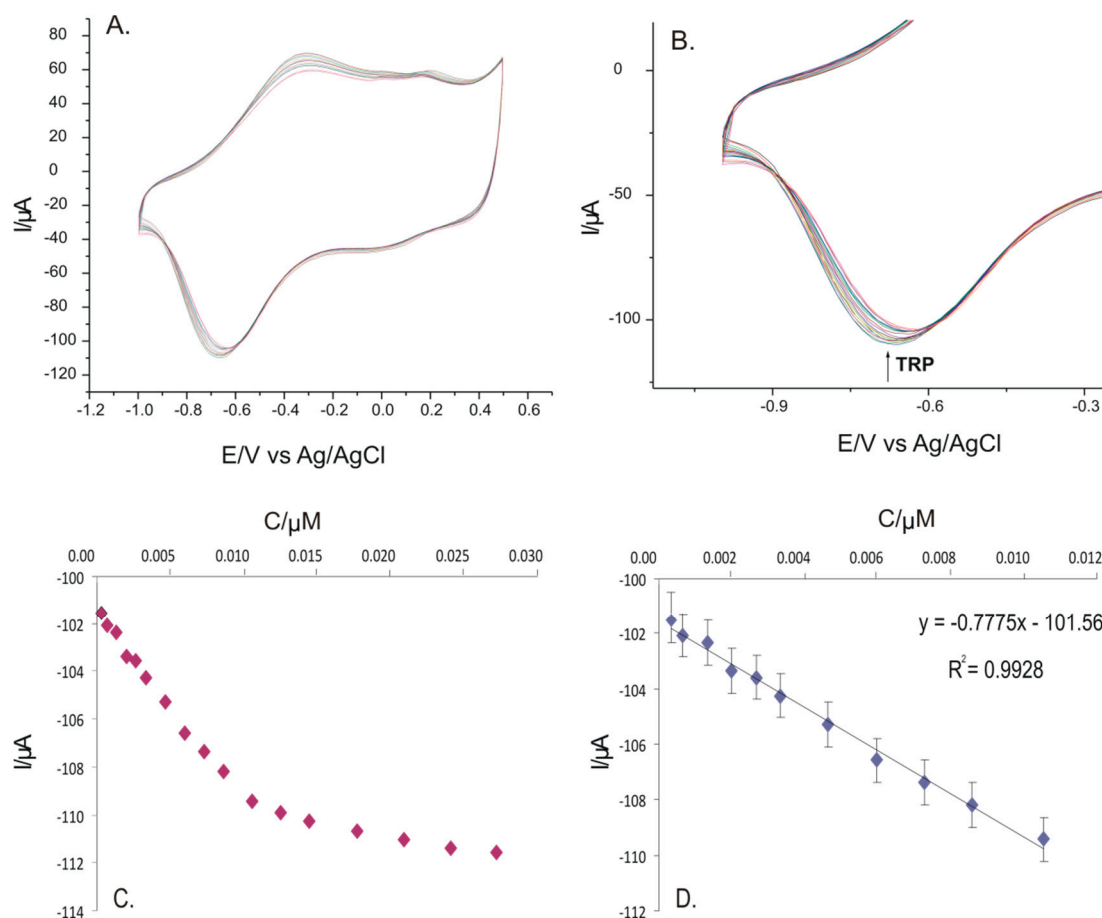

Figure 8. (**A**) Cyclic voltammograms of the PPy/FeCN sensor immersed in a double solution of 0.1 M KCl and 10^{-3} M L-TRP at different concentrations between 3.33×10^{-7} M and 2.72×10^{-5} M. (**B**) Zoomed in image on the catodic peak for which the calibration curve was developed. (**C**) Variation of the current of cathodic peak I with the TRP concentration. (**D**) Calibration curve in the range between 3.3×10^{-7} M and 1.06×10^{-5} M.

Table 4. LOD and LOQ obtained with the PPy/FeCN sensor detecting L-TRP.

Sensor	LOD [1] (M)	LOQ [2] (M)
PPy/FeCN-SPCE	1.05×10^{-7}	3.51×10^{-7}

[1] Limit of detection. [2] Limit of quantification.

The LOD and LOQ were calculated using the slope of the calibration equation and the standard deviation of the sensor response in a blank solution [38].

The detection limit obtained with the PPy/FeCN sensor was lower than the sensor's LODs presented in Table 2, making it possible to be used for the sensitive detection of L-TRP from pharmaceutical samples.

3.5. Method Precision, Stability and Reproducibility

Precision studies performed for the Ppy/FeCN sensor were performed both interday and intraday, based on solutions with L-TRP contents alongside the concentration of 5×10^{-6} M. The interday precision was evaluated on 4 distinct days, and the intraday precision was analyzed in 3 different moments of the day at an interval of 2 h. The relative standard deviation (RSD (%)) presented the following values: 4.2% interday and 3.8%

intraday. The good stability of the Ppy/FeCN sensor, both in the short and long term, was demonstrated by the CV method. In the short term, there were 30 consecutive scans recorded with the sensor developed in a double solution of 5×10^{-5} M L-TRP–0.1 M KCl, keeping the intensity of the peaks at 97.8% compared with the initial response. In the long term, there 96% stability out of the initial response was obtained after 5 days, with the RSD representing a value of 95%.

In addition, the sensor's reproductibility was created in a double solution of 5×10^{-5} M L-TRP–0.1 M KCl, preparing three different sensors. The RSD value for the cathodic peak observed in all 3 cases was 3.1%.

3.6. Validation of the Modified Sensor by Quantitative Determination of L-TRP in Pharmaceutical Samples

A series of existing products of the pharmaceutical market contains the active compound L-TRP, which is the subject of the present study. Of these, Cebrium and Sleep Optimizer were tested for sensor validation using the FT-IR method, as well as comparing the electroanalytical results with those indicated by the manufacturers. The two pharmaceutical products have different compositions, different concentrations of L-TRP and come from different manufacturers (Cebrium: 1.02 mg L-TRP per capsule, Ever Neuro Pharma; Sleep Optimizer: 150 mg L-TRP per capsule, Solaray).

The L-TRP from the two products was quantified through two methods—CV and FT-IR—where CV was the method developed in this study, and FT-IR was the standard method.

Figure 9 presents the responses of the sensor immersed in solutions of L-TRP obtained from the analyzed pharmaceutical products. The estimated concentration of L-TRP in the solutions was 5×10^{-6} M. It was observed that the signals were in solutions made out of pharmaceutical products, which were influenced by the presence of other substances, especially in the anodic part of the cyclic voltamogram. L-TRP quantification was performed from the cathodic peak current using the calibration linear equation of I vs. c.
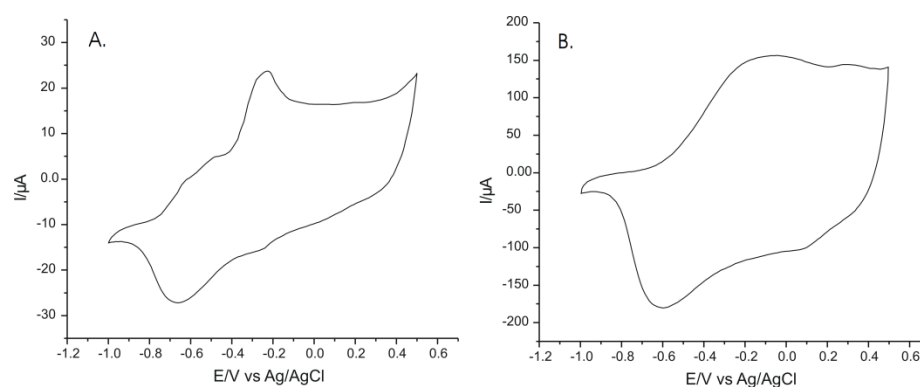

Figure 9. Voltammetric responses of the PPy/FeCN sensor in solutions of (**A**) Cebrium (EVER NEURO PHARMA) and (**B**) Sleep Optimizer (SOLARAY).

For the TRP quantification using the FT-IR method, we used the two solid standards formed of pure TRP and KBr of 1 mg/g and 150 mg/g concentrations, respectively, similar values with those of pharmaceutical products. The absorbance of the 1650 cm^{-1} peak characteristic of the vibration of the N-H group (bending) was used for quantification [43]. The results are presented in Table 5.

Table 5. Quantitative determination of L-TRP in pharmaceutical products.

Pharmaceutical Product	L-TRP Concentration Reported by Producer (mg)	Concentration of L-TRP	
		Method CV ([1]/mg)	Method FT-IR ([2]/mg)
Cebrium EVER NEURO PHARMA	1.02 mg	1.04 ± 0.05	1.06 ± 0.06
Sleep Optimizer SOLARAY	150 mg	150 ± 3	150 ± 4

[1] Cyclic voltammetry. [2] Fourier-transform infrared spectroscopy.

It was observed that the differences between the three sets of values were very small, demonstrating that the quantification method of L-TRP from pharmaceutical products with the sensor had a very good accuracy and could be used in laboratory practice.

4. Conclusions

The CA method proved to be efficient for the PPy doped with FeCN deposition through electropolymerization on an SPCE's surface. The developed sensor in this study, PPy/FeCN/SPCE, presents utility in detecting L-TRP both from model solutions and from pharmaceutical products, showing excellent electroanalytical results, with higher sensibility, precision and good stability. The fast response, low cost and the variety of the fields in which this new device could be applied for the L-TRP, namely the medicine, pharmaceutical, chemistry and food industries, are important advantages for placement in the commercial market, contributing to the control of pharmaceutical products, monitoring some effects caused by an L-TRP deficiency or excess and food quality control.

References

1. Sadok, I.; Tyszczuk-Rotko, K.; Mroczka, R.; Staniszewska, M. Simultaneous voltammetric analysis of tryptophan and kynurenine in culture medium from human cancer cells. *Talanta* **2020**, *209*, 120574. [CrossRef]
2. Liu, X.; Luo, L.; Ding, Y.; Ye, D. Poly-glutamic acid modified carbon nanotube-doped carbon paste electrode for sensitive detection of L-tryptophan. *Bioelectrochemistry* **2011**, *82*, 38–45. [CrossRef] [PubMed]
3. Kagan, J.; Sharon, I.; Béjà, O.; Kuhn, J.C. The tryptophan pathway genes of the Sargasso Sea metagenome: New operon structures and the prevalence of non-operon organization. *Genome Biol.* **2008**, *9*, R20. [CrossRef] [PubMed]

4. Dinu, A.; Apetrei, C. A Review on Electrochemical Sensors and Biosensors Used in Phenylalanine Electroanalysis. *Sensors* **2020**, *20*, 2496. [CrossRef] [PubMed]
5. Yu, L.-Y.; Liu, Q.; Wu, X.-W.; Jiang, X.-Y.; Yu, J.-G.; Chen, X.-Q. Chiral electrochemical recognition of tryptophan enantiomers at a multi-walled carbon nanotube–chitosan composite modified glassy carbon electrode. *RSC Adv.* **2015**, *5*, 98020–98025. [CrossRef]
6. Colombo, S.; Coluccini, C.; Caricato, M.; Gargiulli, C.; Gattuso, G.; Pasini, D. Shape selectivity in the synthesis of chiral macrocyclic amides. *Tetrahedron* **2010**, *66*, 4206–4211. [CrossRef]
7. Caricato, M.; Olmo, A.; Gargiulli, C.; Gattuso, G.; Pasini, D. A 'clicked' macrocyclic probe incorporating Binol as the signalling unit for the chiroptical sensing of anions. *Tetrahedron* **2012**, *68*, 7861–7866. [CrossRef]
8. Kałużna-Czaplińska, J.; Gątarek, P.; Chirumbolo, S.; Chartrand, M.S.; Bjørklund, G. How important is tryptophan in human health? *Crit. Rev. Food Sci. Nutr.* **2019**, *59*, 72–88. [CrossRef] [PubMed]
9. He, Q.; Tian, Y.; Wu, Y.; Liu, J.; Li, G.; Deng, P.; Chen, D. Electrochemical Sensor for Rapid and Sensitive Detection of Tryptophan by a Cu_2O Nanoparticles-Coated Reduced Graphene Oxide Nanocomposite. *Biomolecules* **2019**, *9*, 176. [CrossRef]
10. Heine, W.; Radke, M.; Wutzke, K.-D. The significance of tryptophan in human nutrition. *Amino Acids* **1995**, *9*, 91–205. [CrossRef]
11. Eroğlu, I.; Eroğlu, B.Ç.; Güven, G.S. Altered tryptophan absorption and metabolism could underlie long-term symptoms in survivors of coronavirus disease 2019 (COVID-19). *Nutrition* **2021**, *90*, 111308. [CrossRef]
12. Shaw, K.A.; Turner, J.; Del Mar, C. Tryptophan and 5-Hydroxytryptophan for depression. *Cochrane Database Syst. Rev.* **2002**. [CrossRef]
13. Hudson, C.; Hudson, S.; MacKenzie, J. Protein-source tryptophan as an efficacious treatment for social anxiety disorder: A pilot studyThis article is one of a selection of papers published in this special issue (part 1 of 2) on the Safety and Efficacy of Natural Health Products. *Can. J. Physiol. Pharmacol.* **2007**, *85*, 928–932. [CrossRef] [PubMed]
14. Schneider-Helmert, D.; Spinweber, C.L. Evaluation of L-Tryptophan for Treatment of Insomnia: A Review. *Psychopharmacology* **1986**, *89*. [CrossRef] [PubMed]
15. Mette, C.; Zimmermann, M.; Grabemann, M.; Abdel-Hamid, M.; Uekermann, J.; Biskup, C.S.; Wiltfang, J.; Zepf, F.D.; Kis, B. The impact of acute tryptophan depletion on attentional performance in adult patients with ADHD. *Acta Psychiatr. Scand.* **2013**, *128*, 124–132. [CrossRef]
16. Menkes, D.B.; Coates, D.C.; Fawcett, J.P. Acute tryptophan depletion aggravates premenstrual syndrome. *J. Affect. Disord.* **1994**, *32*, 37–44. [CrossRef]
17. Lovelace, M.D.; Varney, B.; Sundaram, G.; Franco, N.F.; Ng, M.L.; Pai, S.; Lim, C.K.; Guillemin, G.J.; Brew, B.J. Current Evidence for a Role of the Kynurenine Pathway of Tryptophan Metabolism in Multiple Sclerosis. *Front. Immunol.* **2016**, *7*, 246. [CrossRef]
18. Liu, Y.; Tian, A.; Wang, X.; Qi, J.; Wang, F.; Ma, Y.; Ito, Y.; Wei, Y. Fabrication of chiral amino acid ionic liquid modified magnetic multifunctional nanospheres for centrifugal chiral chromatography separation of racemates. *J. Chromatogr. A* **2015**, *1400*, 40–46. [CrossRef] [PubMed]
19. Boulet, L.; Faure, P.; Flore, P.; Montérémal, J.; Ducros, V. Simultaneous determination of tryptophan and 8 metabolites in human plasma by liquid chromatography/tandem mass spectrometry. *J. Chromatogr. B* **2017**, *1054*, 36–43. [CrossRef]
20. Yıldız, C.; Bayraktepe, D.E.; Yazan, Z. Electrochemical low-level detection of l-tryptophan in human urine samples: Use of pencil graphite leads as electrodes for a fast and cost-effective voltammetric method. *Mon. Chem.* **2020**, *151*, 871–879. [CrossRef]
21. Whiley, L.; Nye, L.C.; Grant, I.; Andreas, N.J.; Chappell, K.E.; Sarafian, M.H.; Misra, R.; Plumb, R.S.; Lewis, M.R.; Nicholson, J.K.; et al. Ultrahigh-Performance Liquid Chromatography Tandem Mass Spectrometry with Electrospray Ionization Quantification of Tryptophan Metabolites and Markers of Gut Health in Serum and Plasma—Application to Clinical and Epidemiology Cohorts. *Anal. Chem.* **2019**, *91*, 5207–5216. [CrossRef]
22. Hawkins, G.; Zipkin, I.; Marshall, L. Determination of Uric Acid, Tyrosine, Tryptophan, and Protein in whole Human Parotid Saliva by Ultraviolet Absorption Spectrophotometry. *J. Dent. Res.* **1963**, *42*, 1015–1022. [CrossRef]
23. Fan, Y.; Liu, J.-H.; Lu, H.-T.; Zhang, Q. Electrochemistry and voltammetric determination of L-tryptophan and L-tyrosine using a glassy carbon electrode modified with a Nafion/TiO_2-graphene composite film. *Microchim. Acta* **2011**, *173*, 241–247. [CrossRef]
24. Zhao, J. Simultaneous determination of plasma creatinine, uric acid, kynurenine and tryptophan by high-performance liquid chromatography: Method validation and in application to the assessment of renal function: Simultaneous Determination of Cr, UA, KYN and TRP by HPLC. *Biomed. Chromatogr.* **2015**, *29*, 410–415. [CrossRef] [PubMed]
25. Ritota, M.; Manzi, P. Rapid Determination of Total Tryptophan in Yoghurt by Ultra High Performance Liquid Chromatography with Fluorescence Detection. *Molecules* **2020**, *25*, 5025. [CrossRef] [PubMed]
26. Zhao, M.; Zhou, M.-F.; Feng, H.; Cong, X.-X.; Wang, X.-L. Determination of Tryptophan, Glutathione, and Uric Acid in Human Whole Blood Extract by Capillary Electrophoresis with a One-Step Electrochemically Reduced Graphene Oxide Modified Microelectrode. *Chromatographia* **2016**, *79*, 911–918. [CrossRef]
27. Li, S.; Xing, M.; Wang, H.; Zhang, L.; Zhong, Y.; Chen, L. Determination of tryptophan and tyrosine by chemiluminescence based on a luminol–N-bromosuccinimide–ZnS quantum dots system. *RSC Adv.* **2015**, *5*, 59286–59291. [CrossRef]
28. Moscetti, I.; Cannistraro, S.; Bizzarri, A.R. Probing direct interaction of oncomiR-21-3p with the tumor suppressor p53 by fluorescence, FRET and atomic force spectroscopy. *Arch. Biochem. Biophys.* **2019**, *671*, 35–41. [CrossRef] [PubMed]
29. Viter, R.; Iatsunskyi, I. Metal Oxide Nanostructures in Sensing. In *Nanomaterials Design for Sensing Applications*; Elsevier: Amsterdam, The Netherlands, 2019; pp. 41–91. ISBN 978-0-12-814505-0.

30.　Tığ, G.A. Development of electrochemical sensor for detection of ascorbic acid, dopamine, uric acid and L-tryptophan based on Ag nanoparticles and poly(L-arginine)-graphene oxide composite. *J. Electroanal. Chem.* **2017**, *807*, 19–28. [CrossRef]

31.　Hashkavayi, A.B.; Raoof, J.B.; Park, K.S. Sensitive Electrochemical Detection of Tryptophan Using a Hemin/G-Quadruplex Aptasensor. *Chemosensors* **2020**, *8*, 100. [CrossRef]

32.　Ensafi, A.A.; Hajian, R. Determination of tryptophan and histidine by adsorptive cathodic stripping voltammetry using H-point standard addition method. *Anal. Chim. Acta* **2006**, *580*, 236–243. [CrossRef]

33.　Xia, Y.; Zhao, F.; Zeng, B. A molecularly imprinted copolymer based electrochemical sensor for the highly sensitive detection of L-Tryptophan. *Talanta* **2020**, *206*, 120245. [CrossRef]

34.　He, Q.; Liu, J.; Feng, J.; Wu, Y.; Tian, Y.; Li, G.; Chen, D. Sensitive Voltammetric Sensor for Tryptophan Detection by Using Polyvinylpyrrolidone Functionalized Graphene/GCE. *Nanomaterials* **2020**, *10*, 125. [CrossRef] [PubMed]

35.　Duan, S.; Wang, W.; Yu, C.; Liu, M.; Yu, L. Development of Electrochemical Sensor for Detection of L-Tryptophan Based on Exfoliated Graphene/PEDOT:PSS. *Nano* **2019**, *14*, 1950058. [CrossRef]

36.　Tat'yana, V.V.; Efimov, O.N. Polypyrrole: A Conducting Polymer; Its Synthesis, Properties and Applications. *Russ. Chem. Rev.* **1997**, *66*, 443.

37.　Gniadek, M.; Wichowska, A.; Antos-Bielska, M.; Orlowski, P.; Krzyzowska, M.; Donten, M. Synthesis and characterization of polypyrrole and its composites coatings on flexible surface and its antibacterial properties. *Synth. Met.* **2020**, *266*, 116430. [CrossRef]

38.　Dinu, A.; Apetrei, C. Development of Polypyrrole Modified Screen-Printed Carbon Electrode Based Sensors for Determination of L-Tyrosine in Pharmaceutical Products. *IJMS* **2021**, *22*, 7528. [CrossRef]

39.　Bieńkowski, K.; Strawski, M.; Szklarczyk, M. The determination of the thickness of electrodeposited polymeric films by AFM and electrochemical techniques. *J. Electroanal. Chem.* **2011**, *662*, 196–203. [CrossRef]

40.　Apetrei, C. Novel method based on polypyrrole-modified sensors and emulsions for the evaluation of bitterness in extra virgin olive oils. *Food Res. Int.* **2012**, *48*, 673–680. [CrossRef]

41.　Ghoreishi, S.M.; Behpour, M.; Ghoreishi, F.S.; Mousavi, S. Voltammetric determination of tryptophan in the presence of uric acid and dopamine using carbon paste electrode modified with multi-walled carbon nanotubes. *Arab. J. Chem.* **2017**, *10*, S1546–S1552. [CrossRef]

42.　Dinu, A.; Apetrei, C. Voltammetric Determination of Phenylalanine Using Chemically Modified Screen-Printed Based Sensors. *Chemosensors* **2020**, *8*, 113. [CrossRef]

43.　Zhang, J.; Wang, D.; Li, Y. Ratiometric Electrochemical Sensors Associated with Self-Cleaning Electrodes for Simultaneous Detection of Adrenaline, Serotonin, and Tryptophan. *ACS Appl. Mater. Interfaces* **2019**, *11*, 13557–13563. [CrossRef] [PubMed]